De novo Design and Characterization of Copper Centers in Synthetic Four-Helix-Bundle Proteins

Robert Schnepf,[†,‡] Patric Hörth,[†] Eckhard Bill,[‡] Karl Wieghardt,[‡] Peter Hildebrandt,[‡] and Wolfgang Haehnel[†,*]

Contribution from the Albert-Ludwigs-Universität Freiburg, Institut für Biologie II/Biochemie, Schänzlestrasse 1, D-79104 Freiburg, Germany, and Max-Planck-Institut für Strahlenchemie, Stiftstrasse 34-36, D-45470 Mülheim a. d. Ruhr, Germany

Received May 30, 2000. Revised Manuscript Received December 9, 2000

Abstract: The design and chemical synthesis of *de novo* metalloproteins on cellulose membranes with the structure of an antiparallel four-helix bundle is described. All possible combinations of three different sets of amphiphilic helices were assembled on cyclic peptide templates which were bound by a cleavable linker to the cellulose. In the hydrophobic interior, the four-helix bundle proteins carry a cysteine and several histidines at various positions for copper ligation. This approach was used successfully to synthesize, for the first time, copper proteins based on a four-helix bundle. UV−vis spectra monitored on the solid support showed ligation of copper(II) by about one-third out of the 96 synthesized proteins and tetrahedral complexes of cobalt(II) by most of these proteins. Three of the most stable copper-binding proteins were synthesized in solution and their structural properties analyzed by spectroscopic methods. Circular dichroism, one-dimensional NMR, and size-exclusion chromatography indicate a folding into a compact state containing a high degree of secondary structure with a reasonably ordered hydrophobic core. They displayed UV−vis absorption, resonance Raman, and EPR spectra intermediate between those of type 1 and type 2 copper centers. The present approach provides a sound basis for further optimizing the copper binding and its functional properties by using combinatorial protein chemistry guided by rational principles.

Introduction

The design of a new or modified metal site in proteins challenges the understanding of relationships between protein structure and function. A protein-bound metal site consists of one or more metal ions and the amino acid side chain ligands and often an external cofactor providing the first coordination sphere. Strategies to create or to vary metal centers may be summarized in three classes. Modification of natural metalloproteins by site-directed mutagenesis is successful in particular to disclose the function of individual amino acids.[1] In addition, this approach has the advantage that the structure of the native protein provides a solid basis to analyze the properties of the modified metal site.

Another approach is the implementation of a metal site into a natural protein that lacks such a site. The ligating amino acid side chains have to be introduced at favorable positions that may be suggested by the aid of molecular modeling. Limitations of the protein design may be overcome by iterative design cycles to get close to the anticipated protein properties as demonstrated by Hellinga,[2] who introduced a new copper center in thioredoxin. However, the extensive procedure imposes serious constraints on the synthesis of a large number of protein variants with potential metal binding sites.

A third possibility is the chemical synthesis of *de novo* proteins to create binding sites for metal ions such as Cu, Ru, Zn, or Co.[3−6] A flexible strategy is to adapt the template-assembled synthetic proteins (TASP)[7] to a combinatorial assembly of the peptide building blocks on cellulose membranes.[8] The template offers the advantage to position and to orient amphipathic helices in an antiparallel four-helix bundle with the hydrophobic regions oriented to the interior of the bundle. This strategy was used successfully to synthesize a large number of heme proteins and to tune their redox potentials as screened spectroscopically on the solid support.[8] This approach promises to constitute a sound basis for the *de novo* design and synthesis of proteins with other metal centers. The strong binding of a Ru ion to bipyridyl ligands attached to a peptide has been used to assemble three helices in parallel orientation.[4] Here, we have utilized the stability of the four-helix bundle itself to provide the scaffold for metal centers with rather weak ligand−metal bonds and ligation by three or four amino acid residues. Creation

* To whom correspondence should be addressed.
† Albert-Ludwigs-Universität Freiburg.
‡ Max-Planck-Institut für Strahlenchemie.

(1) (a) van Pouderoyen, G.; Andrew, C. R.; Loehr, T. M.; Sanders-Loehr, J.; Mazumdar, S.; Hill, H. A. O.; Canters, G. W. *Biochemistry* **1996**, *35*, 1397−1407. (b) Alexander, R. S.; Kiefer, L. L.; Fierke, C. A.; Christianson, D. W. *Biochemistry* **1993**, *32*, 1510−1518.
(2) Hellinga, H. *J. Am. Chem. Soc.* **1998**, *120*, 10055−10066.
(3) Ghadiri, M. R.; Case, M. A. *J. Angew. Chem., Int. Ed.* **1993**, *32*, 1594−1597.
(4) Ghadiri, M. R.; Soares, C.; Choi, C. *J. Am. Chem. Soc.* **1992**, *114*, 825−831.
(5) Handel, T. M.; Williams, S. A.; DeGrado, W. F. *Science* **1993**, *261*, 879−885.
(6) Tuchscherer, G.; Lehmann, C.; Mathieu, M. *J. Angew. Chem., Int. Ed.* **1998**, *37*, 2990−2993.
(7) (a) Mutter, M.; Altmann, E.; Altmann, K. H.; Hersperger, R.; Koziej, P.; Nelbel, K.; Tuchscherer, G.; Vuilleumier, S. *Helv. Chim. Acta* **1988**, *71*, 835−847. (b) Mutter, M.; Tuchscherer, G.; Miller, C.; Altmann, K. H.; Carey, R. I.; Wyss, D. F.; Labhardt, A. M.; Rivier, J. E. *J. Am. Chem. Soc.* **1992**, *114*, 1463−1470. (c) Mutter, M.; Tuchscherer, G. *Cell. Mol. Life Sci.* **1997**, *53*, 851−863.
(8) Rau, H. K.; DeJonge, N.; Haehnel, W. *J. Angew. Chem., Int. Ed.* **2000**, *39*, 250−253.

10.1021/ja001880k CCC: $20.00
Published on Web 02/16/2001

of a specific binding site for a metal ion demands the designing of the liganding amino acid residues in an arrangement that fulfills the geometric requirements of the coordination sphere.

The present work focuses on the *de novo* synthesis of mono copper proteins. In nature, such proteins are involved in biological electron transfer and enzymatic reactions.[9] Mono copper centers in proteins have been classified as type 1 and type 2 according to their spectroscopic and structural properties.[10] Type 1 copper centers are formed by a trigonal ligand set of two His and one Cys and in most cases a weak fourth ligand such as Met forming a distorted tetrahedron. These proteins are also denoted as blue copper proteins due to a relatively strong absorption band at ca. 600 nm that originates from a Cys-S→Cu charge-transfer transition. Natural type 2 copper sites are colorless and have a tetragonal coordination shell formed by the nitrogen and oxygen atoms of the ligands His, Tyr, Asp, or H_2O. Characteristic for type 1 proteins is the small hyperfine splitting of the low-field EPR signal of the copper center ($<100 \times 10^{-4}$ cm^{-1}) while type 2 copper proteins exhibit larger splitting constants ($>160 \times 10^{-4}$ cm^{-1}).[11] Mutational studies with azurin, a blue type 1 copper protein, showed that replacement of a His ligand by Gly causes the transformation to a type 2 or an intermediate state termed type 1.5 as judged from spectroscopic data.[12] This transformation is reflected by a shift of the 600-nm absorption to ca. 400 nm as well as by the substantial frequency lowering of the Cu−S stretching mode in the resonance Raman (RR) spectrum.[12] The relationships between spectroscopic data and structural parameters provide the basis for an efficient analysis of new copper centers.

The *de novo* synthesis of copper proteins described in this work is based on the TASP concept that substantially reduces the folding problem as the branched design constrains the orientation of the individual peptides. Hence, rational design principles can be used to create protein variants with a minimum ligand set of two histidines and one cysteine. Although a structural model can be proposed for template-assembled four-helix bundle proteins, a precise prediction of the ligand arrangement is not possible. Therefore, a large number of proteins with putative copper binding sites were synthesized by a permutative combination of three different sets of peptides. The solid-state synthesis on cellulose allows the in situ screening of the protein variants with respect to their copper binding capabilities using UV−vis absorption spectroscopy. Thus, it is possible to optimize the structural elements that are crucial for the formation of a stable copper binding site.

Experimental Section

Materials. *N*,*N*′-Diisopropylethylamine (DIEA), *o*-(benzotriazol-1-yl)-1,1,3,3-tetramethyluronium tetrafluoroborate (TBTU), 5-(4-(aminomethyl)-3,5-bis(methyloxy)phenoxy)valeric acid/poly(ethylene glycol)/polystyrene (PAL-PEG-PS) resin, and 9-fluorenylmethyloxycarbonyl (Fmoc) protected amino acids were purchased from Perspective Biosystems with the exception of Fmoc-L-Glu(OH)-Oall, Fmoc-β-Ala-OH, and Fmoc-L-Lys(Dde)-OH, which were obtained from Novabiochem. Preloaded Fmoc-GlyNovaSyn TGT resin and modified Rink linker *p*-(*R*,*S*)α-[l-(9H-flouren-9-yl)-methoxyformamido]-2,4-dimethoxybenzyl]phenoxy acetic acid were purchased from Novabiochem, and Whatman 1CHR cellulose sheets were obtained from Merck. All other chemicals were obtained from Aldrich/Sigma or Merck and were of highest available purity grade.

Synthesis of the Templates. The template-helix building block T4-A_h (**4**) (Figure 1) for the cellulose-based protein assembly was synthesized on PAL-PEG-PS resin by using standard Fmoc chemistry. Glu(OH)-OAll was attached to the resin by its γ-carboxyl group to allow on-resin cyclization (**1**→**2**). Amino acids were coupled by TBTU/DIEA except for Cys which was activated as symmetrical anhydride with diisopropylcarbodiimide (DIC).[13] After cleavage of the Fmoc group from the last amino acid Lys(1-(4,4dimethyl-2,6-dioxocyclohex-2-ylidene)ethyl (Dde)) of the linear peptide, the allyl group of Gln1 was cleaved by using $Pd((C_6H_5)_3P)_4$ in 37/2/1 (v/v/v) $CHCl_3$/acetic acid/*N*-methylmorpholine.[14] The head-to-tail cyclization of the decapeptide was performed by reaction of 1 equiv of TBTU and 1 equiv of DIEA in dimethyl formamide (DMF) for 2 h to yield **2**. After removal of the protecting group of Lys (Dde) by treatment with 2/98 (v/v) hydrazine/DMF (**2**→**3**),[15] helix A_h (Figure 2) was synthesized onto ϵ-N(Lys) and the N-terminus acetylated (**3**→**4**) by using a multiple batch solid phase synthesizer (Advanced ChemTech Model 396) as described.[8] The final peptide was cleaved from the resin and purified as described.[8]

The synthesis of the cyclic template T2 (cyclo-[C(SBu^t)-A-C(Trt)-P-G-C(SBu^t)-A-C(Acm)-P-G]) has been described previously.[16]

Synthesis of Helical Building Blocks A_h, B_i, and C_k. The peptides given in Figure 2 were synthesized in a multiple batch solid phase synthesizer (Advanced Chem Tech Model 396) as described above. The final peptides C_k and the variant of A_h for the soluble proteins were acetylated with 5/95 (v/v) acetic anhydride/DMF, followed by removal of the allyl protecting group at the ϵ-amino group of Lys16 as described above. 3-Maleimidopropionic acid was coupled to the N-terminus of peptide B_i and to the ϵ-amino group of Lys16 of C_k and A_h via the symmetrical anhydride as described above. The peptides were deprotected and cleaved with 92/5/3 (v/v/v) trifluoro acetic acid (TFA)/dithiothreitol/anisole except for SBu^t and Acm, precipitated in cold 50/50 (v/v) diethyl ether/*n*-hexane and purified by preparative reversed phase HPLC and analyzed by mass spectrometry as described.[16]

Assembly of the Modular Proteins on Cellulose Membranes. The *mo*dular *p*roteins (Mop) were assembled as described previously,[8] with some modifications. Whatman 1CHR cellulose sheets (7.4 cm × 11.6 cm) were derivatized with β-alanine as described by Frank.[17] The activated modified Rink linker was applied to 48 spots per sheet by using a patterned metal plate as a position marker. Activation was achieved by preparing the *tert*-butyl ester of the linker at a concentration of 0.3 M in DMF via reaction with 1.2 equiv of *tert*-butyl alcohol and 1.2 equiv of DIC for 45 min. Aliquots of 2 μL of the solution were applied to the 48 positions of the sheet resulting in spots 8 mm in diameter. Acetylation of free amino groups, washing, and Fmoc cleavage was carried out as described by Frank.[17] 3-Maleimidopropionic acid was attached to the Rink linker by pipetting 1.4 mL of a 0.15 M solution of the symmetrical anhydride in DMF to each membrane. The amounts of coupling reagents were determined by quantitative Fmoc analysis of a few spots.[18] To monitor the progress of the synthesis, additional control peptides were synthesized on each sheet.

A sample of 150 μL of a solution of building block T4-A_h was prepared by mixing 20 μL of a stock solution of 100 mg/mL T4-A_h in 3/2 (v/v) water/acetonitrile with 100 μL of degassed 2/1 (v/v) 0.25 M sodium phosphate/acetonitrile (pH 8). Immediately after mixing, aliquots of 3 μL of the solution were transferred to each spot at a loading density of approximately 40 nmol/cm^2 (**5**) (Figure 1). After 15 min the sheets were incubated for 15 min in 30 mL of 100 mM sodium phosphate

(9) (a) Sykes, A. G. *Adv. Inorg. Chem.* **1991**, *36*, 377−408. (b) Rydèn, L. *Copper Proteins and Copper Enzymes*; CRC Press: Boca Raton, FL, Lontie, R., Ed.; 1984; Vol. 1, pp 157−182.

(10) Canters, G. W.; Gilardi, G. *FEBS Lett.* **1993**, *325*, 39−48.

(11) Palmer, A. E.; Randall, D. W.; Xu, F.; Solomon, E. I. *J. Am. Chem. Soc.* **1999**, *121*, 7138−7149.

(12) Andrew, C. R.; Yeom, Y.; Valentine, J. S.; Karlsson, G.; Bonander, N.; van Pouderoyen, G.; Canters, G. W.; Loehr, T. M.; Sanders-Loehr, J. *J. Am. Chem. Soc.* **1994**, *116*, 11489−11498.

(13) Atherton, E.; Sheppard, R. C.; Ward, P. *J. Chem. Soc., Perkin Trans. 1* **1985**, 2065−2073.

(14) Kates, S. A.; Daniels, S. B.; Alberico, F. *Anal. Biochem.* **1993**, *212*, 303−310.

(15) Bycroft, B. W.; Chan, W. C.; Chabra, S. R.; Hone, N. D. *J. Chem. Soc., Chem. Commun.* **1993**, 778−779.

(16) Rau, H. K.; DeJonge, N.; Haehnel, W. *Proc. Natl. Acad. Sci.* **1998**, *95*, 11526−11531.

(17) Frank, R. *Tetrahedron* **1992**, *48*, 9217−9232.

(18) Fields, G. B.; Noble, R. L. *Int. J. Peptide Protein Res.* **1990**, *35*, 161−214.

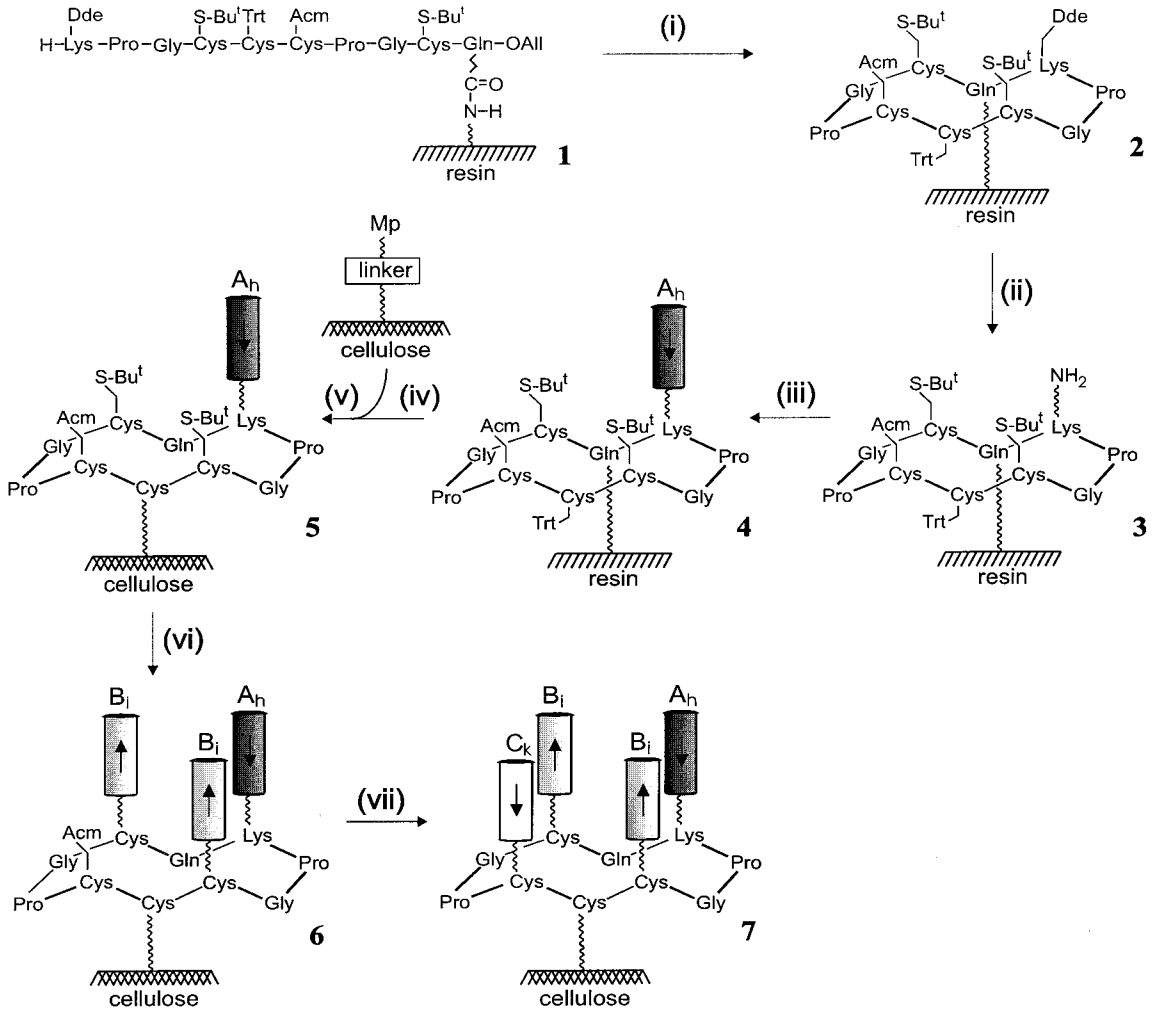

Figure 1. Synthesis scheme of the cyclic decapeptide, the elongation of the helix A at the side chain of Lys of the template, and assembly of the four-helix bundle on the cellulose membrane. The fragment T4-A_h was synthesized on a resin loaded with a peptide amide linker. Synthesis steps: (i) Pd(0) in DCM, TBTU/DIEA in DMF; (ii) hydrazine in DMF; (iii) solid-phase synthesis; (iv) 19/1 TFA/DTT, HPLC; (v) phosphate buffer/acetonitrile (2/1), pH 8; (vi) DTT, pH 7.8, 10 equiv of helix B_i, pH ≈ 8; (vii) $Hg(OAc)_2$, pH 4, 10 equiv of helix C_k, pH ≈ 8, $P(Ph)_3$ in *n*-propanol/buffer, pH 7.8.

buffer (pH 7) containing 250 μL of β-mercaptoethanol to deactivate the excess 3-maleimidopropionyl groups. Subsequently, the SBu^t group of T4-A_h was cleavage by shaking the membranes in a solution of 300 mg of dithiothreitol (DTT) in 0.1 M ammonium hydrogencarbonate (pH 7.8). The sheets were washed three times with 3/97 (v/v) acetic acid in water, three times in 1.5/48.5/50 (v/v/v) acetic acid /water/methanol, and two times with methanol. After drying under reduced pressure, the amount of bound T4-A_h was determined by analyzing the thiol groups of a few spots by the Ellman test.[19] The helices B_i and C_k were attached by chemoselective coupling of their 3-maleimidopropionyl group to the cysteinyl sulfur of the template.

Solutions of 50 mg/mL of helix B_i were prepared by mixing stock solutions of 200 mg/mL of B_i in 3/2 (v/v) water/acetonitrile with 100 μL of degassed 2/1 (v/v) 0.25 M sodium phosphate/acetonitrile (pH 8). Immediately after mixing, 3 μL aliquots of the solution were transferred to the spots of the sheet and allowed to react for 10 min to yield **6**. This procedure was repeated one time. The membranes were washed and dried as described above.

The Acm protecting group was cleaved by shaking the membranes in a solution of 75 mg of mercuric acetate in 15 mL of ammonium acetate (pH 4) for 30 min. Then the sheet was shaken for 3 h with 150 mg of DTT in 0.15 M sodium phosphate (pH 7) and subsequently washed and dried. The building blocks C_k were added to the individual spots of the sheet analogous to the coupling of the other helices to yield (**7**).

To deprotect the Cys residue of helices C_k, the membranes were shaken in 40/54/6 (v/v/v) 0.3 M ammonium acetate/*n*-propanol/tributylphosphine (pH 7.8) for 2 h and washed twice with 20 mL of 3/97 (v/v) acetic acid/*n*-propanol. Afterward the membranes were washed and dried as described above.

All reactions involving reagents with free thiol groups (DTT and β-mercaptoethanol) were carried out under argon in an airtight container to avoid oxidation. To monitor the assembly of the *de novo* proteins by HPLC and mass spectrometry spots with precursors and final products were cut out and cleaved from the membrane by incubation in a solution of 50/45/4/1 (v/v/v/v) TFA/CH_2Cl_2/water/triisopropylsilane for 60 min. The solution was separated from the cellulose and the solvent evaporated under reduced pressure to a final volume of 25 μL. The peptides were precipitated with cold diethyl ether and analyzed. To incorporate copper or cobalt into the proteins, the membranes were shaken in a solution of 1/1 (v/v) water/acetonitrile, washed three times with degassed 100 mM Tris/HCl (pH 7.5), and incubated with a degassed solution of either 1 mM $CuCl_2$ or 1 mM $CoCl_2$ in 100 mM NaCl and 100 mM Tris/HCl (pH 7.5).

Assembly of the Modular Proteins in Solution. The soluble variants of the modular four-helix-bundle proteins Mop5, Mop6, Mop7, and Mop8 were synthesized from template T_2 and the corresponding helices A_h, B_i, and C_k as described and purified by HPLC.[16] Metal incorporation was achieved by addition of defined amounts of a Cu(II) solution.

Size-Exclusion Chromatography. Size-exclusion chromatography was performed on a Hewlett-Packard model 1050 Ti HPLC system

(19) Riddles, P. W.; Blakeley, R. L.; Zerner, B. *Methods Enzymol.* **1983**, *91*, 49−61.

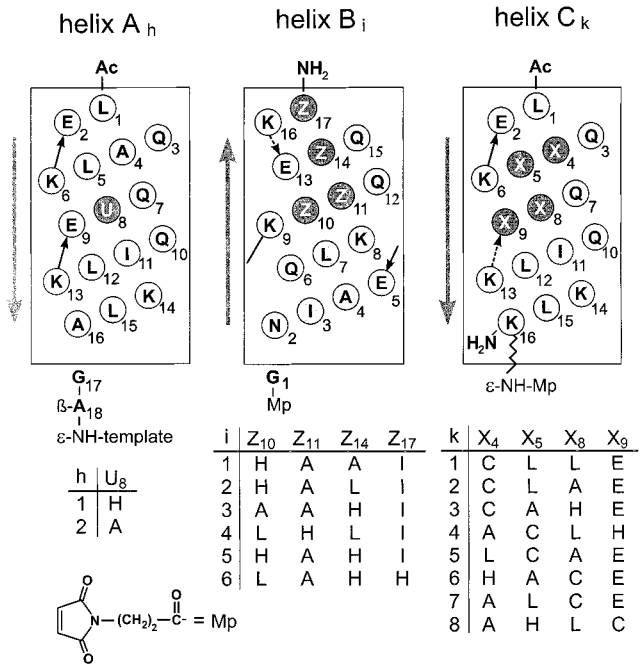

h	U_8
1	H
2	A

i	Z_{10}	Z_{11}	Z_{14}	Z_{17}
1	H	A	A	I
2	H	A	L	I
3	A	A	H	I
4	L	H	L	I
5	H	A	H	I
6	L	A	H	H

k	X_4	X_5	X_8	X_9
1	C	L	L	E
2	C	L	A	E
3	C	A	H	E
4	A	C	L	H
5	L	C	A	E
6	H	A	C	E
7	A	L	C	E
8	A	H	L	C

Figure 2. Helical net representation of the designed helical fragments according to a supercoiled packing. The tables give the index of helices A_h, B_i, and C_k and the amino acid residues at the marked positions U, Z, and X, respectively. Light gray indicates invariant hydrophobic amino acid residues assumed to assemble the hydrophobic core of the four-helix bundles.

equipped with a Pharmacia Superdex 75 column (10 × 300 mm).[8] For the apoproteins, the column was equilibrated with 50 mM Tris (pH 7.5) and 100 mM NaCl. In case of Zn-Mop5, the buffer contained in addition 1 mM $ZnCl_2$. To estimate the molecular mass of the peptides in solution, the column was calibrated with bovine serum albumin (67 kDa), ovalbumin (43 kDa), myoglobin (17.6 kDa), RNase A (13.7 kDa), and aprotinin (6.5 kDa). The peptides applied at a concentration of 150 μM were eluted at a flow rate of 0.5 mL/min and the absorbance was monitored at 215 nm.

UV−Vis Absorption Spectroscopy and Screening. UV−vis spectra of the cellulose-bound metalloproteins in 1 mM $CuCl_2$ or 1 mM $CoCl_2$, 100 mM NaCl, and 100 mM Tris/HCl (pH 7.5) were recorded from 200 to 1000 nm at given times after metal ion addition. The experimental setup included a photodiode array spectrometer (J&M, Germany) and a deuterium and halogen light source that were coupled to the membrane by optical fibers. The spectra were evaluated with respect to the intensity and temporal stability of the absorption bands in the visible region and categorized into three classes for each parameter. UV−vis spectra of the copper proteins in solution were recorded from a 100 μL volume with use of a microcuvette.

Extinction coefficients of the copper proteins were determined by addition of 0.5 equiv of $CuCl_2$ to a protein solution of about 80 μM in degassed 100 mM NaCl and 100 mM Tris/HCl (pH 7.5). Only in the case of Mop5 was $CuCl_2$ added in excess to the protein, the concentration of which was determined by Ellman's test.[19] As the copper protein complexes decompose with time, these extinction coefficients can only be regarded as approximate values.

The dissociation constant of Mop5 was determined from a Scatchard plot of a metal titration experiment. Aliquots of a concentrated $CuCl_2$ solution were added to a protein solution of 80 μM in degassed 100 mM Tris/HCl (pH 7.5). The protein concentration was determined as described above. The data were corrected for the dilution of the solution during the titration.

The dissociation constant and extinction coefficients of the cobalt proteins were determined from a metal titration experiment. Aliquots of a concentrated $CoCl_2$ solution were added to a protein solution of 100 μM in degassed 100 mM Tris/HCl (pH 7.5) and the absorption spectrum was monitored. The protein concentration was determined as described above. The data were corrected for dilution and for absorbance of excessive $CoCl_2$ and fitted to a model of noncooperative Co(II) binding to a protein with a single binding site.

EPR Spectroscopy. X-band EPR spectra of frozen solutions of the copper proteins (50 μM protein, 15 μM $CuCl_2$ in buffer of 100 mM NaCl, 100 mM Tris/HCl, pH 7.5) were recorded on a Bruker ESP 300E spectrometer equipped with a helium flow cryostat (Oxford Instruments ESR 910) at 60 K in a quartz cell (d = 3 mm).

NMR Spectroscopy. ^{1}H NMR data were recorded on a Bruker DRX 400 MHz spectrometer with weak irradiation to saturate residual HOD. Spectra were acquired with protein at a concentration of 400 μM in 20 mM Tris/HCl, pH 7.5, and 10% D_2O at 301 K.

Resonance Raman Spectroscopy. RR spectra were recorded with a double monochromator (2400/mm holographic gratings) equipped with a photomultiplier using the 413 nm line of a krypton ion laser. The spectral bandwidth was 2.8 cm^{-1} and the wavenumber increment 0.5 cm^{-1}. The copper protein complex (1.5 mM protein, 1.5 mM $CuCl_2$ in a buffer of 100 mM NaCl, 100 mM Tris/HCl at pH 7.5) was contained in an EPR tube deposited in a cryostat. The spectra were measured at −140 °C with a laser power of less than 40 mW at the sample.

Circular Dichroism Spectroscopy. CD spectra were recorded with a Jasco 700 spectrometer. The samples with a protein concentration of 10 μM in 10 mM Tris/HCl at pH 7.5 were contained in a quartz cuvette of 1 mm path length. The mean residue molar ellipticity was calculated by dividing the molar ellipticity by the number of residues. Denaturation was performed by guanidine hydrochloride (GuHCl) as described previously,[20] and monitored by CD spectroscopy. The free energy of folding was estimated from a fit of ΔG_{obs} (=ΔG_{H_2O} − m[GuHCl]) to the experimental data.

Results

Design Strategy. The design of the antiparallel four helices is based on the backbone structure of the ROP protein (Protein Data Base 1ROP),[21] a natural supercoiled four-helix bundle. To build the *de novo* structure, most of the amino acids of ROP were replaced by amino acids with a high helical propensity.[22] The linkage of the amphiphilic helices to the peptide template and the association of their hydrophobic faces ensures the position and orientation of the helical segments relative to each other. In addition, the design of the helical peptides (Figure 2) was guided by the heptad repeat,[23] leading to a supercoiled packing of the helices.[24] The folding was further stabilized by a minimized dipole moment of the helices achieved by (i) acetylation of the N-terminus of helices A and C, (ii) amidation of the C-terminus of helices B and C, (iii) N-capping by an Asn residue in the two B helices, and (iv) salt bridges between Glu and Lys spaced by four residues in the individual peptides.[25] Within the framework of the protein structure, His residues and a single Cys were positioned as potential copper ligands next to each other but at various positions of the helices to create copper sites in the hydrophobic core of the bundle. The residues adjacent to these ligands were varied in size to optimize the hydrophobic packing around the copper site and to prevent oxidation of Cys. Following these design criteria we have synthesized the 96 combinations of 2, 6, and 8 different A_h, B_i, and C_k helices, respectively.

For a cyclo(ABCB) arrangement of the helices, orthogonal protecting groups and linkers were used according to the

(20) Rau, H. K.; Haehnel, W. *J. Am. Chem. Soc.* **1998**, *120*, 468−476.
(21) Banner, D. W.; Kokkinidis, M.; Tsernoglou, D. *J. Mol. Biol.* **1987**, *196*, 657−675.
(22) (a) O'Neil, K. T.; DeGrado, W. F. *Science* **1990**, *250*, 646−651. (b) Bryson, J. W.; Betz, S. F.; Lu, H. S.; Suich, D. J.; Zhou, H. X.; O'Neil, K. T.; DeGrado, W. F. *Science* **1995**, *270*, 935−941.
(23) Roy, S.; Ratnaswamy, G.; Boice, J. A.; Fairman, R.; McLendon, G.; Hecht, M. H. *J. Am. Chem. Soc.* **1997**, *119*, 5302−5306.
(24) Kamtekar, S.; Hecht, M. H. *FASEB J.* **1995**, *9*, 1013−1022.
(25) Marqusee, S.; Baldwin, R. L. *Proc. Natl. Acad. Sci.* **1987**, *84*, 8898−8902.

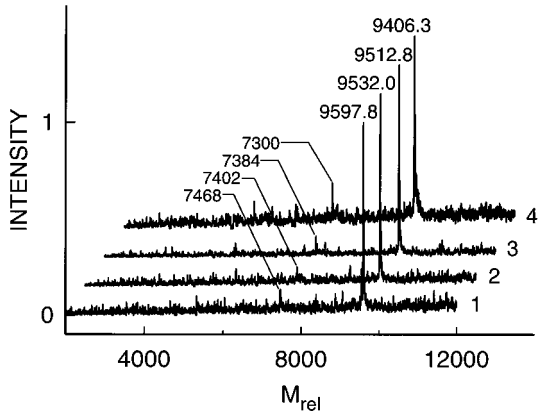

Figure 3. Deconvoluted electrospray mass spectra of four-helix bundle proteins after cleavage from cutout spots and precipitation with diethyl ether. The traces 1−4 correspond to the four-helix bundles $T_4A_1(B_4)_2C_6$, $T_4A_2(B_4)_2C_6$, $T_4A_1(B_2)_2C_6$, and $T_4A_1(B_1)_2C_5$, respectively. The masses reveal the correct primary structure of the template assembled four-helix bundle proteins. Only minor contributions of the three-helix bundle without helix C_k were detected and are labeled by their mass.

following strategy: (i) cyclization of the resin-bound template after deprotection of Allyl at the α-carboxyl group of Glu by Pd(0), orthogonal to all protecting groups in (**1**); (ii) selective extension of the template at Lys(Dde) by helix A at the resin after deprotection of Dde by 2% hydrazine, orthogonal to Trt, SBu^t, Acm, and the linker at the resin; (iii) cleavage from resin, deprotection of helix A and Cys(Trt) of the template by TFA, orthogonal to SBu^t and Acm; (iv) attachment of the template with helix A to cellulose via Cys to maleimidopropionic acid bound to the TFA sensitive Rink-linker; (v) coupling of two helices B after deprotection of Cys(SBu^t), orthogonal to Acm and the Rink-linker; (vi) coupling of helix C carrying a new SBu^t-protected Cys for Cu-ligation after deprotection of Cys-(Acm), orthogonal to Rink-linker; (vii) deprotection of the Cu-liganding Cys by $P(Ph)_3$, orthogonal to the linker; and (viii) for tests of the complete proteins cleavage of Rink-linker by TFA.

Figure 3 shows ESI mass spectra of four of the modularly assembled proteins after cleavage from the cellulose membrane without purification. The main peak of the spectra confirms the correct assembly and the purity of the proteins. Impurities resulting from incomplete coupling of the last helix C_k contribute less than 10% to the spectra and are labeled by their mass.

UV−Vis Absorption Spectroscopy and Screening. The formation of a copper−protein complex can be monitored by the relatively strong Cys(S)→Cu(II) charge transfer (CT) transitions between 350 and 650 nm. Therefore, at several time intervals after $CuCl_2$ addition, the UV−vis spectra were measured in the range from 200 to 1000 nm from all spots of cellulose-bound proteins. The intensity of an absorption band and its time-dependent decay revealed the binding of Cu and the stability of the complex. Figure 4 shows a qualitative summary of the results. About 30% of the 96 proteins exhibited a CT band characteristic for copper binding. The arrangement in a matrix displays the effect of amino acid variations in the individual helices. In particular, it reveals that all four helical segments contribute to the formation of the copper binding site. For most of the Cu(II)-binding proteins, the CT-absorption band disappeared within a few minutes. The Cys residues of these Cu complexes are oxidized as checked by determination of the free thiol groups using Ellman's reagent.[19] For the most stable copper proteins, the CT band was found at ca. 400 nm indicating a dominant (S→Cu) $\sigma\rightarrow\pi^*$ CT transition and a distorted tetragonal Cu site. The *mo*dular *p*rotein with the helix composition $T_4A_2(B_2)_2C_7$, denoted as Mop5, was that with the highest long-term stability. This protein as well as Mop6 ($T_4A_2(B_1)_2C_7$), Mop7 ($T_4A_2(B_5)_2C_2$), and Mop8 ($T_4A_2(B_2)_2C_6$) were synthesized in solution for further spectroscopic characterization (Table 1). In the soluble variants helix A was bound by Mp at the ϵ-amino group of Lys16 to template T_2 with Cys at the position of Lys of the cellulose-bound template T_4. The two linkages of helix A to the template have similar length and are compared in Figure 5.

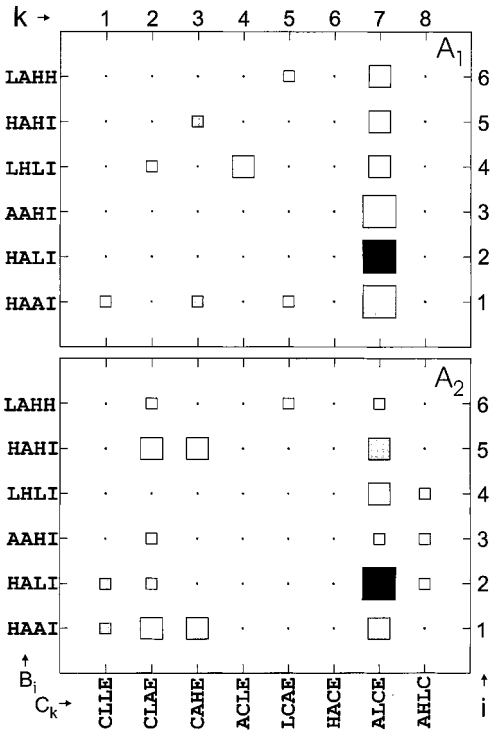

Figure 4. Matrix representation of the absorption properties of the copper protein complexes. The size of the squares gives three categories of the intensity of the CT absorption band. The color of the squares indicate that the CT band in the visible region of the spectrum could be observed for up to 3 min (white), 7 min (gray), and 15 min (black). The data were obtained from spectra measured after addition of a solution of 1 mM $Cu^{II}Cl_2$ in 50 mM Tris (pH 7.5), 100 mM NaCl at 25 °C to the cellulose bound proteines. The top and the bottom matrix refer to proteins with the helices A_1 and A_2, respectively.

Table 1. Molecular Masses of Soluble Apoproteins Determined by ESI Mass Spectrometry

protein	assembled modules	calcd av mass	exptl mass
Mop5	$T_2A_2(B_2)_2C_7$	9237.6	9236.6 ± 0.4
Mop6	$T_2A_2(B_1)_2C_7$	9153.4	9154.6 ± 1.3
Mop7	$T_2A_2(B_5)_2C_2$	9285.5	9287.6 ± 1.0
Mop8	$T_2A_2(B_2)_2C_6$	9261.5	9263.9 ± 1.7

Figure 6 compares the UV−vis spectra of Mop5, Mop6, and Mop7 with their cellulose-bound variants and indicates that for each protein the position and shape of the 400-nm absorption band is the same in the bound and the soluble form (Table 2). Between 550 and 650 nm, however, the cellulose-bound proteins display additional absorption bands which are not observed or, as in Mop7, are substantially altered for the soluble variants. These differences are not likely to be caused by impurities or a heterogeneous protein composition of the cellulose-bound proteins. The almost negligible amounts of three-helix bundle variants detected in Figure 3 lack helix C_k with the copper ligating Cys and can therefore not contribute to the UV−vis absorption in the region above 400 nm. Copper binding was not detected for the soluble and the cellulose-bound Mop8.

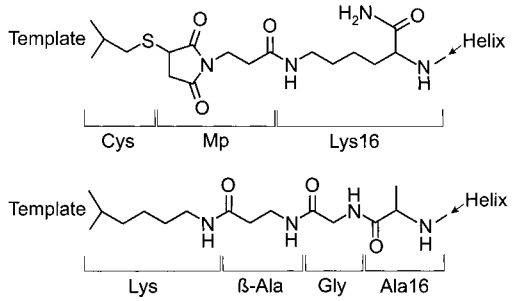

Figure 5. Linker between the template and helix A in the soluble (top) and the cellulose-bound proteins (bottom). Amino acid residues 1 through 15 are the same in the two variants.

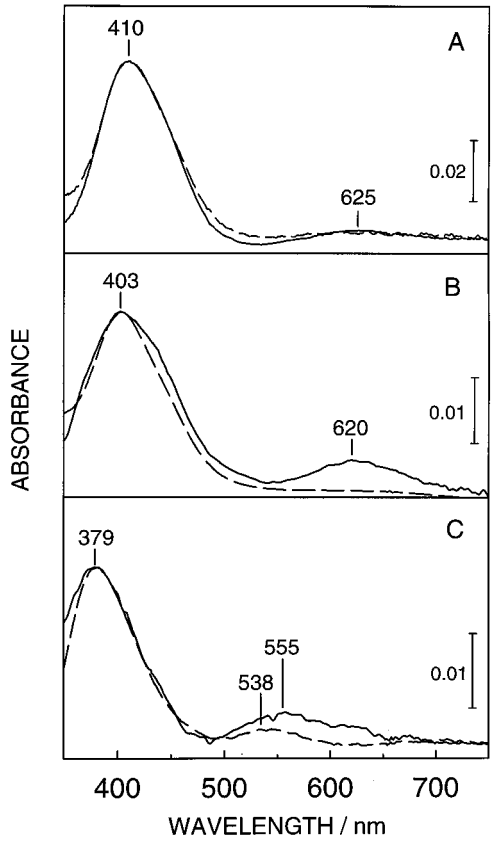

Figure 6. UV−vis absorption spectra of the Cu(II) complexes of Mop5 (**A**), Mop6 (**B**), and Mop7 (**C**) on a cellulose membrane (solid lines) and in solution (dashed lines) measured at 25 °C. The solutions contained 100 mM NaCl (pH 7.5), 50 mM Tris (pH 7.5), 40 μM $Cu^{II}Cl_2$ for Mop5, 12 μM $Cu^{II}Cl_2$ for Mop6, and 10 μM $Cu^{II}Cl_2$ for Mop7 at protein concentrations of 44 μM Mop5 and 20 μM of Mop6 and Mop7. The spectra monitored on the solid phase were normalized to the solution spectra.

Table 2. Absorption, EPR, and Raman Spectroscopic Properties of Copper(II) Complexes in Solution

	absorption (S → Cu CT)	EPR (X-band)		RR
Cu(II) complex	λ_{max}/nm	g_z	$A_z/10^{-4}$ cm^{-1}	ν(Cu−S)/cm^{-1}
Mop5	410	2.189	102	326.5
Mop6	403	2.192	100	nd[a]
Mop7	379	2.175	136	nd[a]
$Cu(II)Cl_2$ in Tris		2.23	200	

[a] Not determined.

Cobalt Proteins. Possible metal-binding sites in the cellulose-bound proteins were also tested by incubation with Co(II) instead of Cu(II). Co(II) was found to form complexes with most of the proteins as indicated by absorption bands around 320 nm and near 600 nm. Figure 7 shows the spectra of Mop5. They are essentially the same for the soluble and the cellulose-bound form. The band at 320 nm originates from a Cys(S)→Co CT transition,[26] that at around 600−650 nm from d→d transitions of tetrahedrally coordinated Co(II).[27] No bands were observed in the range of 400−500 nm as expected for penta- or hexacoordinated complexes. Similar absorption spectra have been reported for Co(II) derivatives of natural blue copper proteins.[28] The Co(II)-binding capability of the protein variants as well as the stability of the complexes is estimated from the intensity and time-dependent change of the 600-nm absorption band (Figure 8). The dissociation constants which were determined by metal titration experiments are substantially higher than those of Cu(II) binding (Table 3). Both the larger number of Co(II) protein complexes and their higher stability as compared to the corresponding Cu(II) complexes may be due to the fact that Co(II) is not capable of oxidizing cysteine residues. The results demonstrate that most of the designed proteins indeed meet the geometrical requirements for a tetrahedral metal binding site.

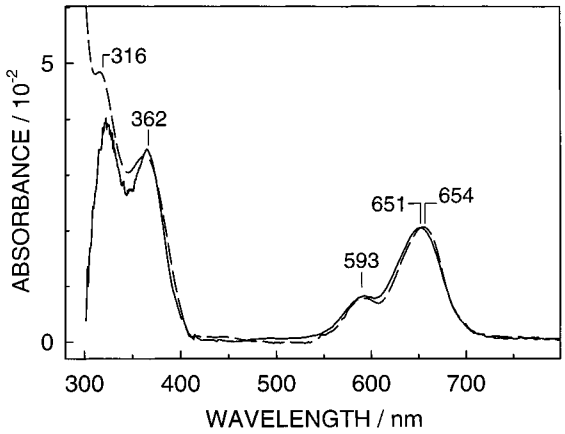

Figure 7. UV−vis absorption spectra of the Co(II) complexes of Mop5 on a cellulose membrane (solid line) and in solution (dashed line) at a concentration of 60 μM and 20 equiv of $CoCl_2$, measured at 25 °C. The solutions contained 100 mM NaCl (pH 7.5) and 50 mM Tris (pH 7.5). Absorbance of excessive $CoCl_2$ has been subtracted.

To investigate zinc binding 1 equiv of $ZnCl_2$ was added to the cobalt complex of Mop5, Mop6, Mop7, and Mop8. The characteristic absorption bands of the cobalt proteins disappeared immediately after addition of Zn(II), indicating a much higher affinity for Zn(II) than for Co(II). Similar results were obtained after addition of Zn(II) to proteins with bound Cu(II), implying that the dissociation constant for the metal complexes increases in the order Zn(II) < Cu(II) < Co(II). This finding is in line with previous results for *de novo* proteins with similar ligand sets.[29]

Dissociation Constant and Extinction Coefficient. The extinction coefficients of the 400-nm absorption bands were estimated for Mop5, Mop6, and Mop7 by addition of $CuCl_2$ to a protein solution with a concentration determined by the Ellman's test.[19] The respective values were 2.04, 2.06, and 2.63 mM^{-1} cm^{-1}, which are comparable to those found for natural copper proteins and mutants containing Cys-coordinated cop-

(26) Bertini, I.; Luchinat, C. *Adv. Inorg. Chem.* **1985**, *6*, 71−111.
(27) (a) Salgado, J.; Jiménez, H. R.; Moratal, J. M.; Kroes, S.; Warmerdam, G. C. M.; Canters, G. W.*Biochemistry* **1996**, *35*, 1810−1819. (b) McMillin, D. R.; Rosemberg, R. C.; Gray, H. B. *Proc. Natl. Acad. Sci.* **1974**, *71*, 4760−4762.
(28) Alexander, R. S.; Kiefer, L. L.; Fierke, C. A.; Christianson, D. W. *Biochemistry* **1993**, *32*, 1510−1518.
(29) Klemba, M.; Regan, L. *Biochemistry* **1995**, *34*, 10094−10100.

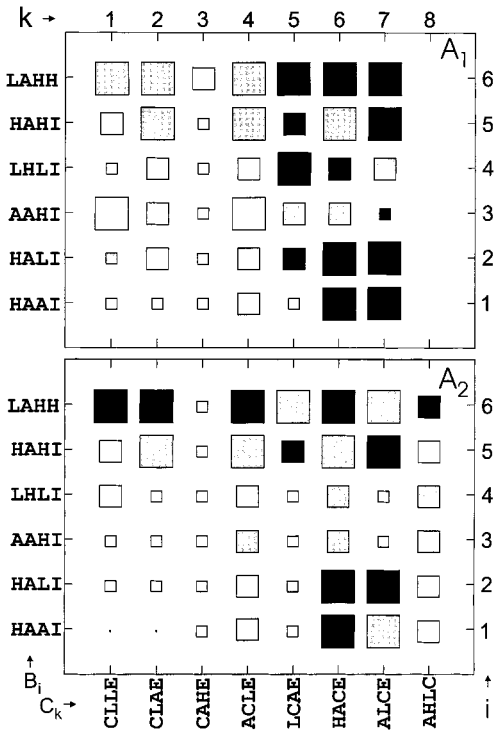

Figure 8. Matrix representation of absorption properties of the Co(II) protein complexes. The size of the squares gives three categories of the intensity of the absorption bands. The color of the squares indicates that the absorption band in the visible region of the spectrum remained unchanged for up to 15 min (white), up to 120 min (gray), and more than 120 min (black). The data were obtained from spectra measured after addition of a solution of 1 mM $Co^{II}Cl_2$ in 50 mM Tris (pH 7.5) and 100 mM NaCl at 25 °C to cellulose bound proteines. The top and the bottom matrix refer to proteins with helices A_1 and A_2, respectively. Proteins with helices A_1 and C_8 were not synthesized.

Table 3. Absorption Spectroscopic Properties of Cobalt(II) Complexes in Solution

Co(II) complex	λ/nm	ϵ/M^{-1}·cm^{-1}	K_{Diss}Co(II)/μM
Mop5	650	329	355
Mop6	645	nd[a]	>1000
Mop7	623	336	81
Mop8	623	214	481

[a] Not determined.

per.[12] To the stable Mop5 5 equiv and to Mop6 and Mop7 only 0.5 equiv of Cu(II) were added to minimize the oxidation of Cys in the latter two proteins.

The protein solution of Mop5 was titrated with aliquots of concentrated $CuCl_2$ solution. Cu(II) binding was monitored by UV−vis spectroscopy and analyzed by a Scatchard plot (Figure 9). The dissociation constant of 10 μM indicates a tight and specific binding of Cu(II). Furthermore, the Scatchard plot indicates that Cu(II) is bound stoichiometrically and that no other intermediate is formed up to a molar Cu(II)/protein ratio of 1:1.

Size-Exclusion Chromatography. A possible aggregation of the proteins was analyzed by size exclusion chromatography shown in Figure 10. The apoprotein Mop5 elutes at an apparent molecular mass of 12 kDa (11.4 kDa was found in an independent set of runs) and Mop5 with bound Zn at 10.5 kDa, which are in good agreement with a monomeric state. The deviation from the actual mass of 9.2 kDa is attributed to the nonglobular shape of the four-helix bundle in contrast to that of the proteins used for calibration.[30] The symmetric elution

(30) Feng, Y.; Sligar, S. G. *Biochemistry* **1991**, *30*, 10150−10155.

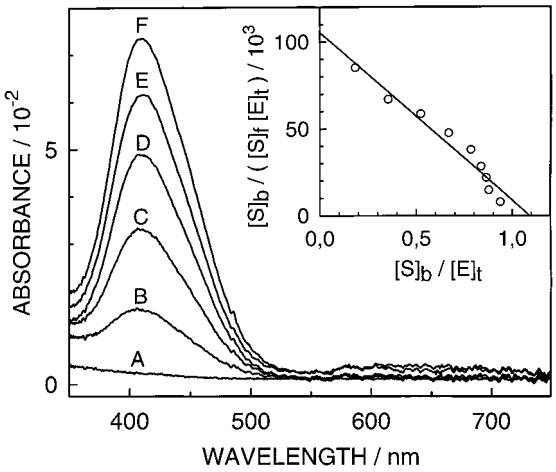

Figure 9. UV−vis absorption spectra of the Cu(II) complex of Mop5 monitoring the titration of the apoprotein at an initial concentration of 44 μM and different concentrations of Cu(II) (A, 0 μM; B, 10 μM; C, 20 μM; D, 30 μM; E, 40 μM; F, 60 μM) in 50 mM Tris (pH 7.5) and 100 mM NaCl. The spectra were corrected for dilution. The inset shows the Scatchard plot obtained from the titration experiment (K_d = 10 μM, n = 1.1).

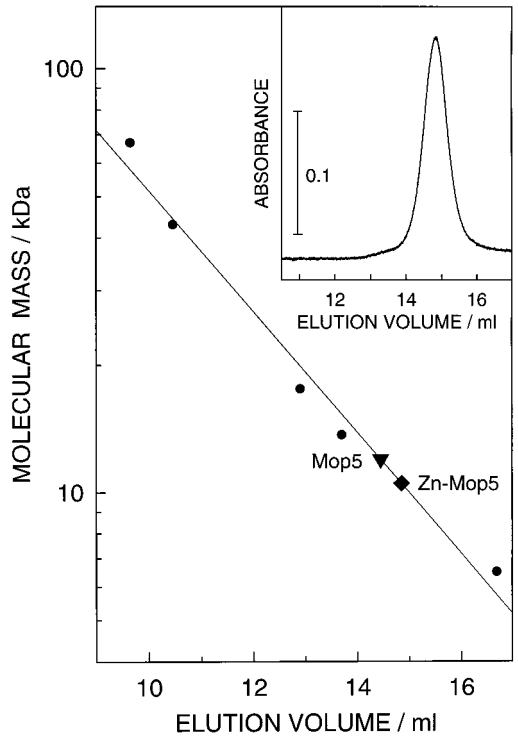

Figure 10. Size-exclusion chromatography of Mop5 (▼) and Zn-Mop5 (◆) at a concentration of 150 μM in 50 mM Tris (pH 7.5) and 100 mM NaCl and a set of globular proteins (●). The elution volumes of Mop5 and Zn-Mop5 indicate a molecular mass of 12 and 10.5 kDa, respectively. The inset shows the size-exclusion chromatogram of Zn-Mop5 in the presence of 1 mM $ZnCl_2$ monitored at 215 nm.

profile shown in the inset of Figure 10 was also found for the apoprotein (not shown) and rules out the formation of dimers or oligomers. Similar results were obtained for Mop6, Mop7, and Mop8.

Circular Dichroism Spectroscopy and Protein Stability. The CD spectra of Mop5 and its Cu(II) complex show minima at 208 and 222 nm and a maximum at 195 nm (Figure 11A), which are characteristic for an α-helical structure. A value of −23000 deg cm^2 $dmol^{-1}$ is determined for the ellipticity at 222 nm. This finding indicates a helical content of 64 and 71% based

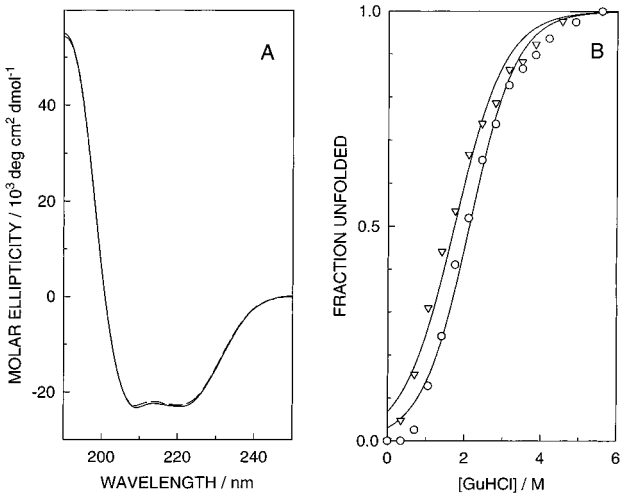

Figure 11. (A) CD spectra of apo-Mop5 (dashed line) and the Cu(II) complex of Mop5 (solid line) between 190 and 250 nm at a concentration of 10 μM in 10 mM Tris (pH 7.5), 20 mM NaCl, and 10 μM $CuCl_2$. (B) Guanidine hydrochloride (GuHCl) denaturation curves for apo-Mop5 (∇) and the zinc complex ($\bigcirc$) monitored by CD spectroscopy at 222 nm at a concentration of $\approx$10 μM in 20 mM Tris (pH 7.5), 20 mM NaCl, and 20 μM $ZnCl_2$. The unfolded fraction is plotted as a function of the concentration of GuHCl. A two-state transition model was fitted to the data (solid line).

on an ellipticity of -35700 and -32200 deg cm^2 dmol^{-1}, respectively, for a pure α-helical protein.[31,32] This result is in good agreement with the fraction of amino acids in the helical sections of the presumed structure. The CD spectra do not indicate significant structural changes upon binding of Cu(II), Co(II), and Zn(II). For Mop6, Mop7, and Mop8 apoproteins, the ellipticities were in the same range as that of Mop5.

Denaturation with GuHCl was monitored by CD spectroscopy for the apoprotein of Mop5 and its Zn(II) complex. Zn(II) was used instead of Cu(II) to avoid interference between the unfolding of the protein and the Cu(II)-induced cysteine oxidation. Both the apoprotein and the Zn complex of Mop5 reveal a cooperative transition upon addition of GuHCl (Figure 11B). Fitting a two-state transition model to the data yields *m*-values of -3.7 and -4.1 kJ/mol/M and a free energy of folding ΔG_{H_2O} of -8.6 and -6.5 kJ/mol for the zinc complex and the apoprotein, respectively. The values are consistent with those expected for proteins with a relatively small hydrophobic core.[4] The deviation of the fit of a simple two-state model from the data in particular at high GuHCl concentrations may result from the effect of template/linker on the unfolding process of the short peptides. However, since the transition midpoints are at 1.7 and 2.1 M GuHCl for the apo- and Zn-protein, respectively, it can be concluded that metal binding increases the structural stability of the four-helix bundle protein.

NMR Spectroscopy. To evaluate the global conformational specificity of Mop5 the chemical shift dispersity was measured in the amide−aromatic proton region and is shown in Figure 12. The resonances are rather broad, but show a good dispersion of chemical shifts for an α-helical structure. A line broadening by aggregation was ruled out since the gel permeation studies show only monomers. Our modular design includes a decapeptide template and linkers to ensure the predetermined assembly

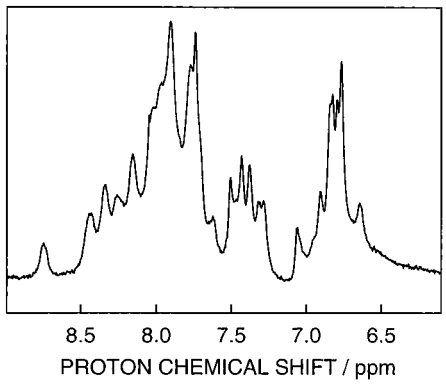

Figure 12. One-dimensional ^{1}H NMR spectrum in the aromatic amide proton region of the apo-Mop5 protein. Experimental conditions are given in the Experimental Section. Chemical shifts are given in parts per million from DSS.

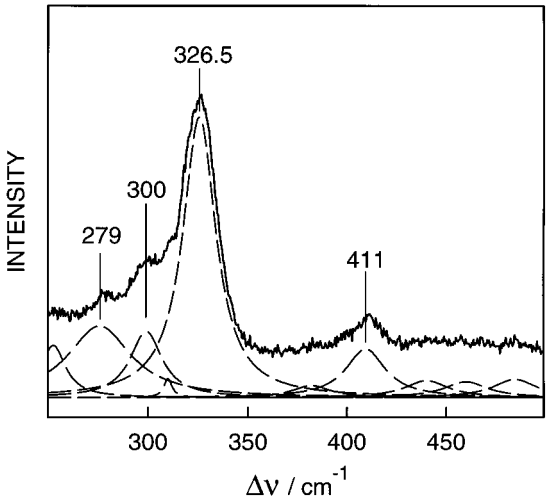

Figure 13. Resonance Raman spectrum of the Cu(II) complex of Mop5 at a concentration of 1.5 mM in 100 mM Tris (pH 7.5), 100 mM NaCl, and 1.5 mM $CuCl_2$ at -140 °C. The excitation line was 413 nm. The fitted Lorentzian line shapes are indicated by the dashed lines.

of the short helices which may have a less defined structure than the helical domain of the molecule. However, the resonances are resolved to a similar extent as those of four-helix bundles designed previously for improved packing of the hydrophobic core.[33]

Resonance Raman Spectroscopy. An excitation frequency in resonance with the S(Cys)→Cu(II) CT transition provides a selective enhancement of the vibrational modes involving internal coordinates of the Cu(II)−cysteine moiety. The strongest resonance enhancement is expected for the mode including the largest contribution of the Cu−S stretching.[34] The RR spectrum of the Cu(II) complex of Mop5, excited at 413 nm (Figure 13), reveals a prominent band at 326.5 cm^{-1}, which is assigned to a mode dominated by the Cu−S stretching. Based on empirical relationships derived from natural copper proteins, this frequency indicates a Cu−S bond length of 2.24 Å.[35] Further RR bands at 279, 300, and 411 cm^{-1} are relatively weak and most likely originate from modes involving internal coordinates of the Cys ligand.

(31) Lau, S. Y. M.; Taneja, A. K.; Hodges, R. S. *J. Biol. Chem.* **1984**, *259*, 13253−13261.
(32) Chen, Y. H.; Yang, J. T.; Chau, K. H. *Biochemistry* **1974**, *13*, 3350−3359.
(33) (a) Betz, S. F.; DeGrado, W. F. *Biochemistry* **1996**, *35*, 6955−6962. (b) Gibney, B. R.; Rabanal, F.; Skalicky, J. J.; Wand, A. J.; Dutton, P. L. *J. Am. Chem. Soc.* **1999**, *121*, 4952−4960.
(34) Qiu, D.; Dasgupta, S.; Kozlowski, P. M.; Goddard, W. A.; Spiro, T. G. *J. Am. Chem. Soc.* **1998**, *120*, 12791−12797.
(35) Andrew, C. R.; Sanders-Loehr, J. *Acc. Chem. Res.* **1996**, *29*, 365−372.

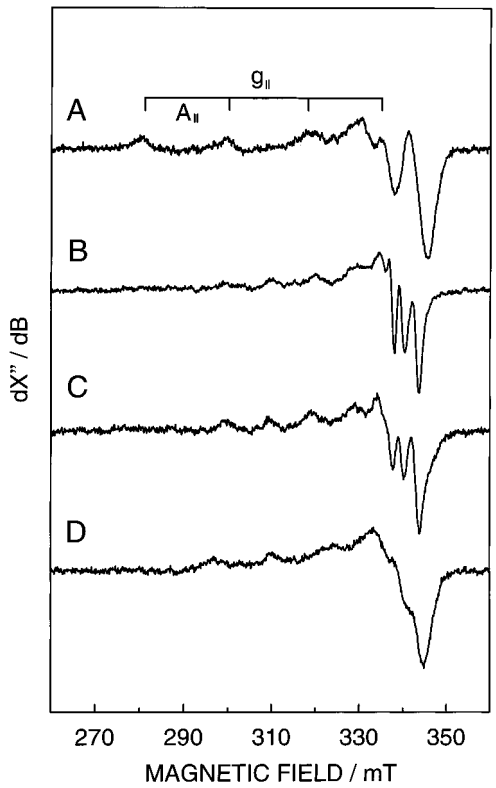

Figure 14. X-band EPR spectra of $Cu(II)Cl_2$ (A) and the Cu(II) complexes of Mop5 (B), Mop6 (C), and Mop7 (D) in 50 mM Tris (pH 7.5) and 100 mM NaCl at 60 K. Experimental conditions: microwave frequency (A) 9.6431, (B) 9.6457, (C) 9.6414, and (D) 9.6428 GHz, microwave power 5 mW, modulation amplitude 12.8 G.

Electron Paramagnetic Resonance Spectroscopy. The EPR spectra of the Cu(II) complexes of Mop5, Mop6, and Mop7 (Figure 14) reveal *g*-values of 2.189, 2.192, and 2.175, and hyperfine splitting constants A_z of 102, 100, and 136 $\times$ 10^{-4} cm^{-1}, respectively (Table 2). The values are in the range observed for various copper proteins,[12] and are distinctly lower than those of $CuCl_2$ dissolved in Tris buffer ($g_z = 2.23$; $A_z = 200 \times 10^{-4}$ cm^{-1}). Therefore, these data indicate specific Cu(II) binding sites in Mop5, Mop6, and Mop7. In particular, the decrease of the g_z values can be rationalized in terms of a geometric distortion exerted by the Cys coordination as well as a higher covalency of the Cu−S bond.[36] The less pronounced coupling of the unpaired electron to the nucleus, which is reflected by the ground-state orbital sensitive A_z value, is characteristic for the anticipated electron delocalization to the sulfur in the synthetic proteins as compared to Cu(II) in buffer.

A linear relationship has been observed between g_z and A_z values for various type 1, type 2, and type 1.5 copper sites, which can be displayed in a Blumberg−Peisach−Vänngard plot.[12,37] Based on these data a type 1.5 copper site can be inferred for Mop5 and Mop6, a type 2 copper site for Mop7.

Discussion

Creating a Copper Binding Site in a Four-Helix Bundle Protein. For the *de novo* design of a metalloprotein with weak metal-to-ligand bonds the stability of the folded apoprotein is an essential objective. A stable fold is achieved by an antiparallel four-helix bundle,[38] in particular, if the association to a defined topology is controlled by the branched architecture of the TASP.[39] This approach has been proven to be successful for the *de novo* design of heme proteins.[20] However, natural soluble mono-copper proteins consist largely of β-sheets.[9] Structural features such as helix bundle motives have not been found in natural mono-copper proteins. Thus, to adapt the stable fold of a synthetic four-helix bundle to a copper protein, a true *de novo* design is needed. Only the His_2/Cys ligation motif was adopted from natural copper proteins. Assuming a packing of the four amphiphilic helices to form a hydrophobic center of the antiparallel bundle the ligating amino acid residues were positioned close enough to each other to form a metal center. We have investigated positions of the complex in the center and close to the open end of the template assembled bundle. The critical distances of the ligands necessary for a metal center have also been varied by changes of neighboring residues which modify the packing of the helices. As demonstrated by the formation of stable Co complexes with a large number of the permutative combinations of the helices (Figure 8) this rational design was successful to position the outer-sphere ligands. However, the rather small number of stable Cu complexes found with these proteins (Figure 4) indicates additional structural requirements for stable Cu complexes. In particular, the thermodynamically favored oxidation of the thiol side chain of Cys by Cu(II) has to be avoided.[2] A stable Cu(II)−thiolate complex can only be formed if the free energy of coordination matches that of thiol exposure to the solvent and its oxidation. The selection of four-helix bundles with a copper center has to meet the requirement that stable folding of the hydrophobic core protects the single Cys from oxidation under aerobic conditions and the formation of dimers. This is in agreement with the monomers observed by gel-permeation chromatography in Figure 10. It is also consistent with the good chemical shift dispersity in the amide region (Figure 12).

The design of Cu proteins with a single Cys residue in an antiparallel four-helix bundle is only possible with at least three different helices. In the case of a symmetrical antiparallel helix bundle as used for heme proteins,[8] the two Cys could form inter- or intramolecular S−S bridges. Therefore, the template-assisted protein design was extended, for the first time, to a combinatorial approach with three different helices which provides also a substantially increased number of protein variants over that with two helices.

Properties of the New Copper Proteins. The protein Mop5 was found to be more stable toward Cys oxidation than other proteins with similar sequences. A comparison of the properties of all 96 proteins synthesized in this work indicates structural parameters that control appropriate copper ligation.

(i) Mop5 ($T_4A_2(B_2)_2C_7$) is one of the proteins with the copper site in the center of the four-helix bundle well buried in a hydrophobic core. In proteins such as $T_4A_h(B_i)_2C_k$ ($k = 1-5$) the copper site is localized close to the upper end of the four-helix bundle where partial unfolding may provide free access to the metal binding site and facilitate Cys side chain oxidation.

(ii) Hydrophilic amino acid residues in the hydrophobic core destabilize hydrophobic helix packing and may unshield the putative copper binding site. This might be the reason for the

(36) Solomon, E. I.; Baldwin, M. J.; Lowery, M. D. *Chem. Rev.* **1992**, *92*, 521−542.

(37) (a) Vänngard, T. *Biological Application of Electron Spin Resonance*; Swartz, H. M., Bolton, J. R., Borg, D. C., Eds.; Wiley-Interscience: New York, 1972; pp 411−417. (b) Peisach, J.; Blumberg, W. E. *Arch. Biochem. Biophys.* **1974**, *165*, 691−708.

(38) (a) Schafmeister, C. E.; Miercke, L. J. W.; Stroud, R. M. *Science* **1993**, *262*, 734−738. (b) Kamtekar, S.; Schiffer, J. M.; Xiong, H.; Babik, J. M.; Hecht, M. H. *Science* **1993**, *262*, 1680−1685. (c) Harbury, P. B.; Plecs, J. J.; Tidor, B.; Alber, T.; Kim, P. S. *Science* **1998**, *282*, 1462−1467.

(39) Mutter, M.; Vuilleumier, S. *Angew. Chem.* **1989**, *101*, 551−571.

lack of copper binding in $T_4A_2(B_i)_2C_6$ as compared to $T_4A_2(B_i)_2C_7$, although Co(II) is bound by both proteins in a tetrahedral coordination as judged from UV−vis spectroscopy.

(iii) Mop6 differs from Mop5 by only one amino acid residue at the position Z_{14} of helix B_1 and B_2 one turn above the copper site (cf. Figure 2). But the stability of the Cu(II) complex of Mop5 is substantially higher than that of Mop6. Presumably, the two Leu residues in Mop5 compensate for a bulging of the helical bundle at the Cu(II) coordination site, which may not be possible by the two Ala in Mop6. Leu may also provide a better shielding of the Cys than Ala to prevent access of the solvent.

Structure of the Copper Binding Sites. The CD spectra of Mop5, Mop6, and Mop7 are consistent with an α-helical structure of 80% expected from the structural model. Since binding of zinc to Mop5 stabilizes this structure by not more than 2.1 kJ/mol, copper binding should also increase the protein stability with a rather low contribution to the free energy of folding in the absence of denaturant ΔG_{H_2O} of −6.5 kJ/mol.

UV−vis absorption, RR, and EPR spectroscopy can provide information about the geometry of the coordination sphere and help to identify proteins with copper binding sites of type 1, 1.5, and 2.[1] Type 1 copper proteins are typified by a trigonal His_2Cys ligand set and show a strong absorption band at ca. 600 nm that originates from a (S→Cu) $\pi\rightarrow\pi^*$ CT transition. The second (S→Cu) $\sigma\rightarrow\pi^*$ CT transition of type 1 copper sites is generally very weak except for rhombically distorted complexes where the copper ion moves out of the His_2Cys plane. In these complexes, the $\sigma\rightarrow\pi^*$ CT transition gives rise to an additional relatively strong absorption band at ca. 460 nm. This transition shifts to higher energies and gains intensity at the expense of the $\pi\rightarrow\pi^*$ CT transition in tetragonal complexes which are characterized by a dominant absorption band at ca. 400 nm.

In solution and on the solid support, the Cu(II) complexes of Mop5, Mop6, and Mop7 reveal strong absorption bands at 410, 401, and 379 nm, respectively, indicating tetragonal coordination spheres. In such a geometry, the Cu−S bond is elongated as compared to type 1 copper proteins leading to a downshift of the Cu−S stretching vibration by up to 100 cm^{-1} to ca. 320 cm^{-1}.[12] Indeed, the RR spectrum of the Cu(II) complex of Mop5 displays a strong band at 326.5 cm^{-1}, which in analogy to the His117Gly variant of azurin is assigned to the Cu−S stretching.

For the Cu(II) complexes of Mop5, Mop6, and Mop7, the EPR hyperfine splitting constants A_z are found to be at the lower end of the scale typically observed for type 2 copper proteins and close to those of type 1.5 complexes. In both types of copper complexes, four ligands form a tetragonal donor set with a planar (type 2) or tetrahedrally distorted coordination geometry (type 1.5). Thus, the EPR spectroscopic data indicate tetragonal binding sites with only minor structural differences between the three species in agreement with the results obtained by UV−vis and RR spectroscopy. All three species provide the minimum His_2Cys ligand set and the fourth position could be occupied by an exogenous ligand (e.g. water, hydroxide), backbone nitrogen or oxygen, or an appropriate amino acid side chain (e.g. Lys, Gln, or Glu).

On the other hand, the spectroscopic findings rule out a type 1 binding site in which two His and one Cys occupy three almost equivalent equatorial positions and possibly one or two further ligands weakly bound at the axial positions. A tetragonal coordination geometry seems to be sterically more demanding than a trigonal binding site. Mop5, Mop6, and Mop7 must exhibit a sufficiently high structural flexibility to accommodate a tetragonal binding site, which is also the preferred coordination geometry of Cu(II) complexes in solution. It is concluded that the stabilization of a trigonal binding site, which involves a relatively short Cu−S(Cys) bond distance, requires a precise positioning and rigid fixation of the equatorial His and Cys ligands and the potential axial ligands in the protein matrix.

The absorption spectra of the membrane-attached Cu(II) complexes of Mop5, Mop6, and Mop7 exhibit weak but clearly detectable absorption bands in the region between 550 and 650 nm, attributable to $\pi\rightarrow\pi^*$ CT transitions. These absorption bands are smaller or even missing in the spectra of the soluble complexes. These differences may originate from the slightly different linkage of helix A in the two variants (cf. Figure 5) or reflect interactions at the cellulose matrix which could cause a more rigid four-helix bundle structure as compared to that of the soluble proteins.

Conclusions

We have developed a strategy for the *de novo* design of copper proteins by combining rational design principles with the advantages of combinatorial protein assembly. The assembly of polypeptide building blocks to form proteins on a cellulose membrane in high purity is a prerequisite for synthesizing and screening a large number of protein variants. The TASP concept has been proven to be particularly useful for extending the modular synthesis of the antiparallel four-helix bundle proteins to three different peptides as it is required for the arrangement of the His_2Cys ligands. In contrast to many other combinatorial approaches, the template-assisted synthesis imposes rigorous constraints on the peptide orientation yielding protein variants of defined topology. Thus, it is also possible to derive a realistic structural model of the four-helix bundle protein that constitutes the basis for the rational protein design. We have also shown that the properties of the cellulose-bound proteins are conserved to a large extent in the soluble variants.

Using this approach we succeeded for the first time to synthesize copper proteins based on a four-helix bundle structural motif. The structural properties of the copper binding sites as revealed by different spectroscopic techniques indicate that these proteins accommodate tetragonal coordination geometries with structures between those of a planar (type 2) and a tetrahedrally distorted (type 1.5) binding site. The combinatorial protein chemistry guided by rational principles represents an efficient approach to the *de novo* design and synthesis of metalloproteins. In view of the functional versatility of this class of proteins, the present results constitute an important step toward tailor-made enzymes.

Acknowledgment. Support by the Volkswagen-Stiftung to W. Haehnel and by the Deutsche Forschungsgemeinschaft to P. Hildebrandt is gratefully acknowledged.

JA001880K